Marine Genomics 27 (2016) 47–55

Contents lists available at ScienceDirect

Marine Genomics

Cells to Shells: The genomics of mollusc exoskeletons

Characterisation of the mantle transcriptome and biomineralisation genes in the blunt-gaper clam, *Mya truncata*

Victoria A. Sleight [a,*], Michael A.S. Thorne [a], Lloyd S. Peck [a], Jaison Arivalagan [b,c], Sophie Berland [b], Arul Marie [c], Melody S. Clark [a]

[a] British Antarctic Survey, Natural Environment Research Council, High Cross, Madingley Road, Cambridge CB3 0ET, UK
[b] UMR 7245 CNRS/MNHN Molécules de Communications et Adaptations des Micro-organismes, Sorbonne Universités, Muséum National d'Histoire Naturelle, Paris 75005, France
[c] UMR 7208 CNRS/MNHN/UPMC/IRD Biologie des Organismes Aquatiques et Ecosystèmes, Sorbonne Universités, Muséum National d'Histoire Naturelle, Paris 75005, France

ARTICLE INFO

Article history:
Received 30 September 2015
Received in revised form 28 December 2015
Accepted 7 January 2016
Available online 14 January 2016

Keywords:
Gene expression
Calcification
Phylogenetics
Bioinformatics
Shell

ABSTRACT

Members of the Myidae family are ecologically and economically important, but there is currently very little molecular data on these species. The present study sequenced and assembled the mantle transcriptome of *Mya truncata* from the North West coast of Scotland and identified candidate biomineralisation genes. RNA-Seq reads were assembled to create 20,106 contigs in a de novo transciptome, 18.81% of which were assigned putative functions using BLAST sequence similarity searching (cuttoff E-value 1E−10). The most highly expressed genes were compared to the Antarctic clam (*Laternula elliptica*) and showed that many of the dominant biological functions (muscle contraction, energy production, biomineralisation) in the mantle were conserved. There were however, differences in the constitutive expression of heat shock proteins, which were possibly due to the *M. truncata* sampling location being at a relatively low latitude, and hence relatively warm, in terms of the global distribution of the species. Phylogenetic analyses of the Tyrosinase proteins from *M. truncata* showed a gene expansion which was absent in *L. elliptica*. The tissue distribution expression patterns of putative biomineralisation genes were investigated using quantitative PCR, all genes showed a mantle specific expression pattern supporting their hypothesised role in shell secretion. The present study provides some preliminary insights into how clams from different environments – temperate versus polar – build their shells. In addition, the transcriptome data provides a valuable resource for future comparative studies investigating biomineralisation.

1. Introduction

Biomineralisation is an essential biological process for many living organisms. From microalgae to shellfish, multiple taxa – in at least 30 phyla – secrete calcium carbonate crystals onto a protein matrix (Addadi and Weiner, 1997). The Mollusca is one such phylum whose success since the base of the Cambrian (545 million years ago) is partly attributed to the possession of a hard shell (Jackson et al., 2010; Marie et al., 2013; Vermeij, 2005). The mollusc shell has been the subject of scientific interest for centuries and continues to be researched from increasingly multi-disciplinary perspectives (Marin and Luquet, 2004; Zhang et al., 2012). Shells contain approximately 95–99% calcium carbonate ($CaCO_3$) and 1–5% organic matrix; the organic component is a protein matrix which applies synergetic forces that either nucleate or inhibit crystal growth (Marie et al., 2010; Meenakshi et al., 1971; Weiner and Hood, 1975). The protein matrix is secreted by the mantle and recently, particularly since the 'omics era began, much research has focussed on understanding the molecular mechanisms of shell growth — specifically the genetic control of shell matrix protein secretion (Clark et al., 2010; Werner et al., 2013; Zhang et al., 2012).

Mya truncata is a marine bivalve which is part of the Myidae family of soft-shelled clams. These clams live buried in sediments, both intertidally and subtidally, and are important in many ecosystem functions such as long-term sediment stabilisation, bioturbation and benthopelagic coupling (Queirós et al., 2013). Members of the Myidae family are edible and important economically as a food source and others, such as *Mya arenaria* are invasive (Powers et al., 2006; Sousa et al., 2009). Large infaunal clam species are morphologically similar, and often inhabit similar ecological niches. Clam species from different geographic and environmental locations can therefore provide valuable models for comparing important biological processes over physical gradients — such as temperature (Morley et al., 2007).

Despite being named "soft-shelled" clams, *M. truncata* have a hard shell which is composed of four structurally distinct layers: (i) the outer periostracum (approximately 3 μm and relatively thin); (ii) an outer shell layer of aragonitic granular prisms; (iii) a middle layer of aragonitic crossed lamellar; and (iv) an aragonitic inner layer of complex

* Corresponding author.
E-mail address: viceig15@bas.ac.uk (V.A. Sleight).

http://dx.doi.org/10.1016/j.margen.2016.01.003

crossed lamellar (Fig. 1). In order to better understand the molecular mechanisms which produce *M. truncata*'s shell, transcriptomic sequence data was generated and mined for biomineralisation candidates.

The objectives of the present study were: 1.) Develop a molecular resource to aid the study of biomineralisation in *M. truncata* by sequencing, assembling and putatively annotating its mantle transcriptome. 2.) Identify and further characterise candidate biomineralisation genes in the newly-assembled *M. truncata* mantle transcriptome. 3.) Further characterise possible biomineralisation mechanisms in *M. truncata* by preliminary comparison with another bivalve species living at lower temperatures, the Antarctic clam, *Laternula elliptica.*

2. Method

2.1. M. truncata mantle transcriptome

2.1.1. Animal collection and RNA extraction

M. truncata (n = 9, mean shell length = 64.5 mm) were collected by the NERC Facility for Scientific Diving from Dunstaffnage Bay, North West Scotland in August 2011. Mantle tissue was dissected from each animal and RNA was extracted using TRI reagent (TRIsure) according to manufacturer's instructions (Bioline, UK) and purified on columns (Qiagen, UK).

2.1.2. Sequencing and bioinformatics

The total mantle RNA from nine individuals was pooled prior to sequencing. Pooled RNA was subject to 454 GS FLX Titanium sequencing at Cambridge University Department of Biochemistry Sequencing Centre.

454 reads were assembled into a de novo transcriptome with GS Data Analysis Software (454.com/products/analysis-software/) on default genomic-style parameters, resulting in a total of 20,106 contigs with an average read length of 675 bp. All contigs were compared to the NCBI non-redundant (nr) database (downloaded for in-house use January 2015) using the Basic Local Alignment Search Tool (BLAST) to search for sequence similarity and putative gene annotation (Altschul et al., 1990). The most highly expressed annotated contigs were identified to highlight dominant processes in the mantle at the transcript level. The mantle transcriptomes of *M. truncata* and *L. elliptica* were compared using tBLASTx with default parameters.

Putative biomineralisation genes were identified using keyword searches for candidates which have previously been shown to be associated with shell production and calcification (Table 1). In addition, contigs which were present in the mantle and shell proteome with similarity to biomineralisation domains (Arivalagan et al., 2016 — in this issue) were also included.

2.2. Tyrosinase bivalve phylogeny

Fifteen of the *M. truncata* mantle contigs showed high sequence similarity to Tyrosinase. To understand the evolution of Tyrosinase proteins in *M. truncata*, phylogenetic analyses were carried out. The fifteen *Tyrosinase* transcripts were mapped to a reference Tyrosinase domain (PF00264) and preliminarily aligned using Clustal-W with default parameters (Larkin et al., 2007). The alignment indicated that most contigs

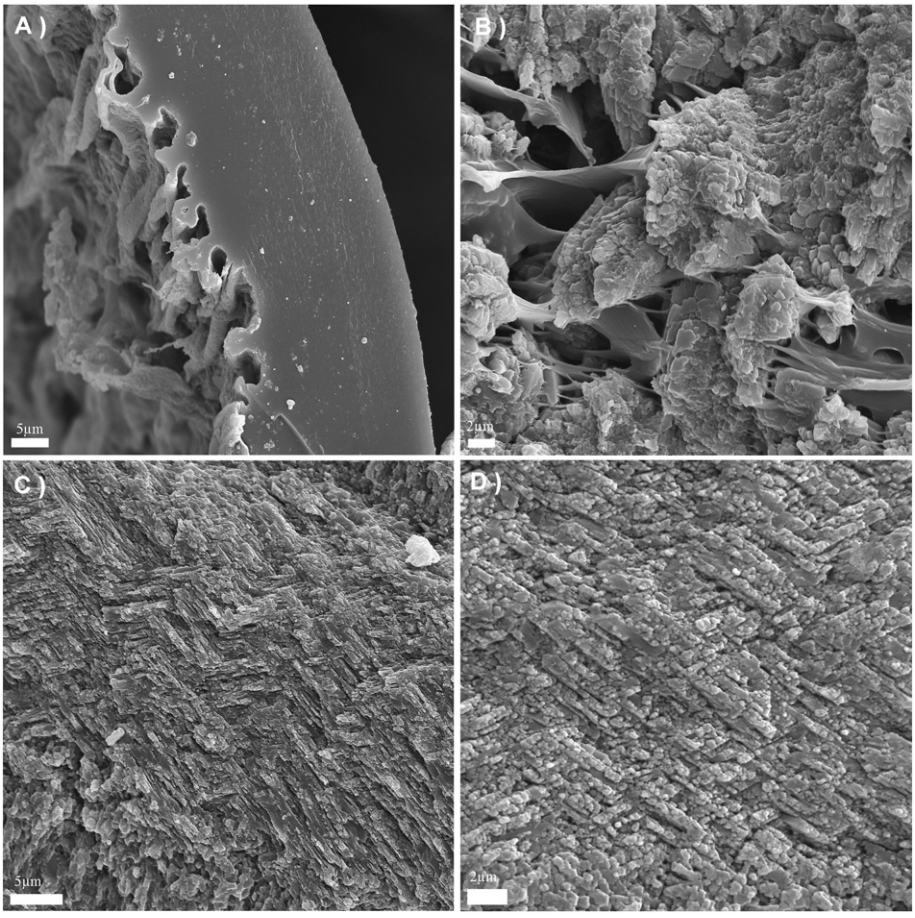

Fig. 1. Microstructural layers of *Mya truncata* shell observed by Scanning Electron Microscopy (SEM). Shells were fractured, ultrasonically cleaned (20 min) and air-dried prior to mounting and sputter coating (3 min, 2 angles; Emitech K550). Observations made using a JEOL JSM-820 SEM. Images courtesy of Elizabeth M. Harper, University of Cambridge. Microstructure nomenclature used as per Bieler et al. (2014). Scale bar on bottom left. A.) Periostracum, B.) outer aragonitic granular prism shell layer, C.) middle aragonitic layer of crossed lamellar and D.) inner aragonitic layer of complex crossed lamellar.

Table 1
Candidate biomineralisation genes selected for tissue distribution analysis, putative annotations and primers used in Q-PCR. "top 50" = in the top 50 most highly expresssed, annotated mantle transcripts, "shell" = present in the shell proteome, "mantle" = present in the mantle proteome, "both" = present in both the shell and mantle proteome.

Contig I.D.	Sequence similarity (BLAST)/ domains (Conserved Domain Database(CDD))	Putative function	Forward and reverse primer sequence (5′ → 3′)	Amplicon size	Annealing temperature (°C)
M. truncata 18s	*M. truncata* 18s	*M. truncata* 18s	GCTCGTAGTTGGATCTCGGG ATCAAGAGCACCAAGGGACG	102	62
Contig0211 (top 50)	Tyrosinase	Biomineralisation	CCCGGGCCTTCTAAATGTGT ACACAACCTTTGTTAACCGGC	103	64
Contig902 (shell)	Tyrosinase	Biomineralisation	CACCCTAATGCGTCAATGGG GACATGAAGGTACCGGGTCA	124	64
Contig629 (both)	Pif	Biomineralisation	CAGTCAGTGTCTGCCAGGTA ACTACATCCACCACAGAGCC	107	64
Contig178 (shell)	Complement control protein domain	Immune/biomineralisation	CTTGCGATCCTGTTCCGAAG TTGCAGGGtTTACACGTGTG	187	64
Contig16470 (both and top 50)	Calponin	Biomineralisation	CGTACCCAGTCATACCCTTCT GGCAAAGATATCAAAGCCGATG	106	64
Contig395 (mantle)	Cartilage matrix-like protein/Von Willebrand factor type A domain	Biomineralisation	CCTCGTTCTTTGCCTCATCG CAGGAATGTTAAGCTCGGCC	236	64
Contig1412 (both)	Chitin-binding domain	Biomineralisation	TTTACTCCCGATGCCAGTGT CTTCGTACCTCCGCAATTGG	222	64

represented gene fragments that mapped to different, non-overlapping regions. To provide the most accurate phylogenetic analysis, only those fragments which overlapped were selected for further analysis. From the initial alignment of fifteen contigs, five were identified as potential paralogues, the remaining eight contigs could still be paralogues, but could not be included in analysis.

The derived amino acid sequences of the five selected contigs were added to a previously published bivalve Tyrosinase alignment (provided by Aguilera et al., 2014) and the phylogeny was determined using the method of Aguilera et al. (2014). Briefly, alignments were created using the MAFFT algorithm (Katoh et al., 2005), refined using the RASCAL webserver (Thompson et al., 2003) and analysed with Gblocks 9.1b (Castresana, 2000) to select conserved regions. The final alignment was used to run three phylogenetic models: Neighbor-Joining (NJ) reconstructions were performed using MEGA 5.2.2 (Tamura et al., 2011), Maximum-likelihood (ML) trees were constructed using RAxMLGUI v. 1.3 (Silvestro and Michalak, 2012) and Bayesian inferences (BIs) were performed using MrBayes v. 3.2 (Ronquist et al., 2012). Data from the three models were manually combined to produce a consensus tree (Fig. 2).

2.3. Tissue distribution of candidate biomineralisation gene expression

2.3.1. Experimental design

Animals (same collection as Section 2.1, n = 5, mean shell length = 60 mm) were dissected into six different tissues: mantle, siphon, gill, foot, digestive gland and gonad. Dissected tissue samples were snap frozen in liquid nitrogen and stored at −80 °C prior to RNA extraction.

2.3.2. RNA extraction and quantitative-PCR

Total RNA was extracted from each tissue of each animal on ice using Tri-Reagent (Bioline, UK) according to manufacturer's instructions, and purified using DNase and RNeasy columns (Qiagen, UK). All RNA samples were analysed for concentration and quality by spectrophotometer (NanoDrop, ND-1000) and tape station analyses (Agilent 2200 TapeStation). All samples were diluted to 30 ng μl^{-1} total RNA, and 30 ng was used to synthesize cDNA following the manufacturer's protocol (Qiagen, QuantiTect Reverse Transcription Kit). cDNA was stored at −20 °C until gene expression analysis.

A total of seven candidate genes were selected for tissue distribution gene expression analysis (Table 1). The *Ribosomal 18s* gene was selected as a housekeeping reference as recommended by previous work on *M. truncata's* sister species — *Mya arenaria* (Siah et al., 2008). Gene-specific primers were designed for unique regions in each candidate using NCBI/Primer-BLAST (Ye et al., 2012) to produce single amplicons with a size of approximately 100–250 bp, an annealing temperature of 62–64 °C and a GC content between 55 and 60%. PCR amplicons were sequenced to confirm identity.

For quantitative PCR (Q-PCR), lyophilised primers (Invitrogen) were reconstituted to 100 μmol with RNase-free water and mixed with Brilliant II SYBR® Green (Agilent, UK) following manufacturer's guidelines. Fluorescence was detected (Stratagene, Mx3000P) over 40 cycles with cycling conditions of 95 °C for denaturing, primer-specific annealing 62–64 °C, and extension at 72 °C. All samples and standards were run in triplicate and each plate included triplicate H_2O and no template controls. Standard curves of each gene were generated on each Q-PCR plate using four point, 2-fold serial dilutions of cDNA (from pooled cDNA). The efficiencies of the Q-PCR reactions were 90–110%, as determined using the slope of the standard curve (Efficiency (%) = [(10(slope / −1)) − 1]).

Quantification of gene expression was conducted using the comparative CT method that normalises the gene expression of each sample in relation to an internal housekeeping gene (*Ribosomal 18s*). Evaluation of CT values for *Ribosomal 18s* across samples indicated it was an appropriate housekeeping gene, ie there was no significant difference in expression across the different tissue types. Normalized CT values were obtained by subtracting the CT value of the internal housekeeping gene from that of the candidate gene in the same sample (ΔCT). Differences between the average ΔCT and ΔCT of each sample were expressed as ΔΔCT. The fold changes ($2^{-\Delta\Delta CT}$) of candidate gene expression were compared across tissues.

2.3.3. Statistics

Data were non-normally distributed (due to the number of zeros or very low values) and could not be transformed to reach normality. Given the non-normal distribution and unbalanced design (mantle n = 5, siphon n = 4, gill n = 5, foot n = 3, digestive gland n = 5, gonad n = 5), data were compared using 95% confidence intervals around the mean average fold change and compared to zero, ie if the confidence interval overlapped with zero (indicating the fold change was equal to zero) or not. For additional stringency, mantle gene expression data were tested against a set median of zero using the non-parametric Wilcoxon Signed Rank Test.

3. Results

3.1. M. truncata mantle transcriptome

RNA-Seq reads from the mantle tissue of nine animals were assembled to create 20,106 contigs in the final de novo transcriptome (reads

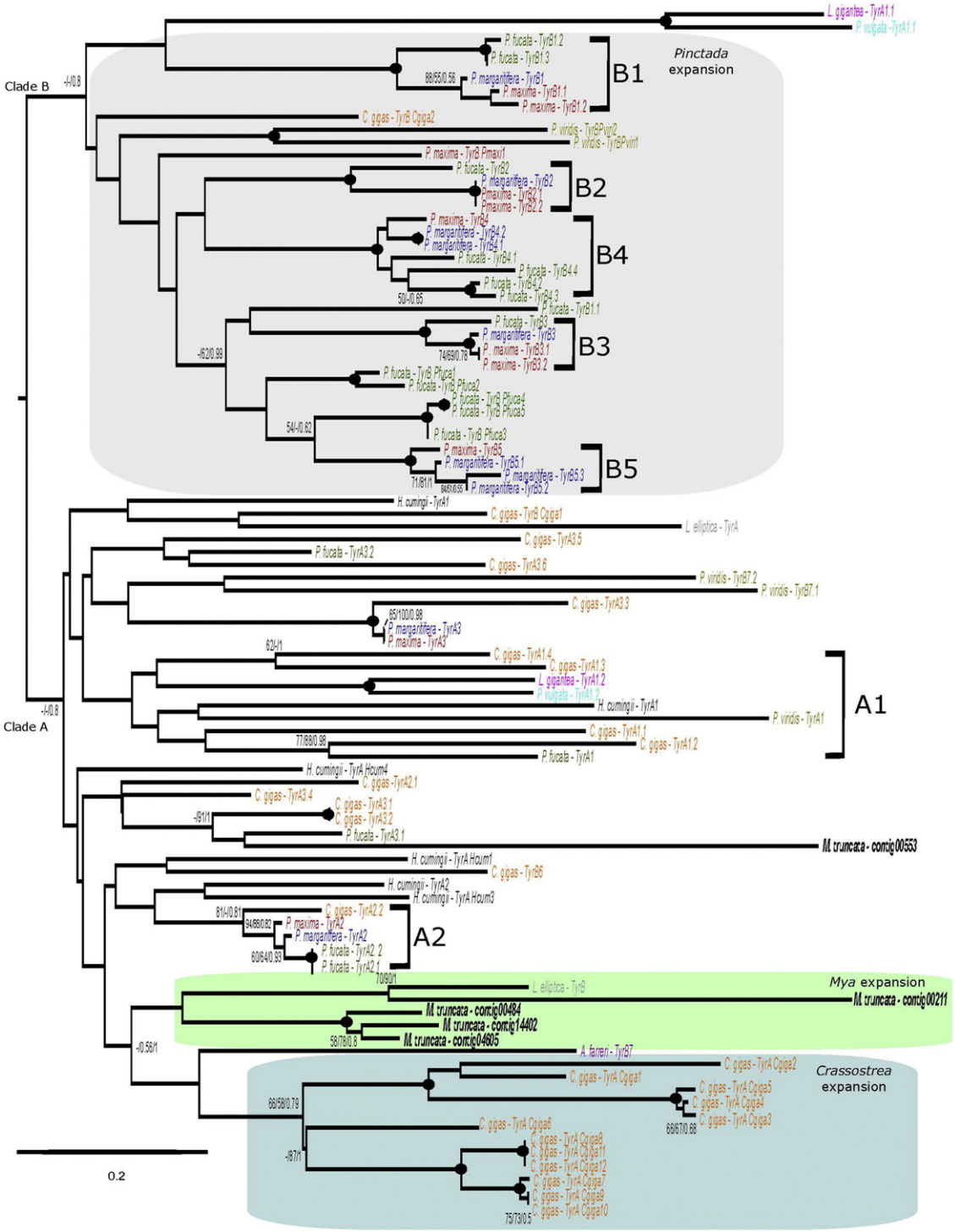

Fig. 2. Phylogenetic analysis of Tyrosinase proteins in shell-building molluscs. A consensus midpoint-rooted tree based on Neighbor-Joining (NJ) topology. Only bootstrap support values >50% and posterior probabilities >0.50, from three different phylogenetic models, are shown at the nodes as follows: NJ bootstrap support/Maximum Likelihood (ML) bootstrap support/Bayesian Posterior Probabilities (BPP). A black dot at the node represents NJ and ML bootstrap >90% and BPP >0.9. Tree labels and nomenclature are consistent with Aguilera et al. (2014) in order to provide an easy visual comparison between the two studies. See Supplementary Figs. 1, 2 and 3 for trees generated from each model.

available from NCBI SRA accession number: SRP064949, assembled contigs available at: http://bit.ly/1QcFiVH). 18.81% of contigs were assigned putative functions using BLAST sequence similarity searching (below an E-value of 1E−10).

The top 50 most highly expressed, annotated, transcripts included many putatively involved in muscle contraction (40%) such as: *Myosin*, *Paramyosin*, *Tubulin*, *Tropomyosin* and *Actin*. Energy production was also a dominant process, with annotation in twelve transcripts (24%), eg *NADH dehydrogenase* and *Cytochrome c oxidase*. Other notable transcripts included three encoding putative biomineralisation genes – *Calponin-3*, *Calponin-2* and *Tyrosinase*; and two chaperone genes – *Heat shock protein 90-alpha 1* and *Heat shock protein 70* (Table 2).

When the mantle transcriptomes of *M. truncata* and *L. elliptica* were compared using tBLASTx, 17.37% of the *M. truncata* contigs showed similarity to an *L. elliptica* contig (below an E-value of 1E−10; Supplementary Table 1). The top 50 most similar contigs included one notable

biomineralisation gene — *Tyrosinase* (Supplementary Table 2). All of the candidate biomineralisation genes selected for Q-PCR also showed strong sequence similarity (below an E-value of 1E−15) to a *L. elliptica* contig (Supplementary Table 2).

3.2. Tyrosinase bivalve phylogeny

At least five putative *Tyrosinase* paralogues were identified in the *M. truncata* mantle transcriptome. The derived amino acid sequences were added to a previously published molluscan Tyrosinase phylogenetic analysis (Aguilera et al., 2014). Many of the nodes had low support values (Fig. 2, Supplementary Figs. 1, 2 and 3), however some reoccurring patterns were observed across the three phylogenetic models used. Two major clades (A & B) were resolved (although it should be noted that there is some confusion in the literature with regards to nomenclature which we believe explains clade discrepancies) in addition to two large, independent expansions in the taxa *Crassostrea* and *Pinctada*. In general the *M. truncata* transcripts clustered in clade A. One of the *M. truncata* transcripts (contig00553) clustered loosely with the *TyrA3* genes from *Crossostrea gigas* and *Pinctada fucata*, whilst all other copies clustered with the *L. elliptica* gene, *TyrB*, and showed evidence of early expansion in the *M. truncata* genome.

3.3. Tissue distribution of biomineralisation gene expression

Seven candidate biomineralisation genes were identified for further analysis based on sequence similarity to known biomineralisation genes, some of which were also present in the top 50 most highly expressed annotated transcripts (Table 2), the shell or mantle proteome (Arivalagan et al., 2016 — in this issue), or any combination of the three (Table 1).

A mantle/siphon-specific signal was detected for all candidates (Fig. 3). None of the mantle 95% confidence intervals overlapped zero and a non-parametric Wilcoxon Signed Rank Test showed that all of the mantle gene expression values were above zero ($P < 0.05$). In contrast, all of

Table 2
The top 50 most highly expressed annotated contigs in the *Mya truncata* mantle transcriptome.

Contig ID	Contig length	No. of reads	Description	Species	Common name	E-value
2653	1206	5190	Paramyosin	*Crassostrea gigas*	Pacific oyster	5.22E−111
270	2488	4806	Myosin heavy chain, striated muscle-like	*Aplysia californica*	Californian sea hare	0
9876	569	3952	Paramyosin	*Mytilus galloprovincialis*	Mediterranean mussel	8.82E−034
1535	1479	3676	Myosin heavy chain	*Placopecten magellanicus*	Atlantic deep-sea scallop	5.00E−141
14488	307	3308	Alpha-L1 nicotinic acetyl choline receptor	*Brugia malayi*	Elephantiasis nematode	5.66E−015
13639	350	3165	Actin	*Marsupenaeus japonicus*	Japanese tiger prawn	9.48E−055
11333	482	2504	Paramyosin	*Mytilus galloprovincialis*	Mediterranean mussel	7.35E−063
8180	661	2106	Actin	*Drosophila persimilis*	Fruit fly	2.14E−071
12700	401	2079	Myosin, regulatory light chain	*Mercenaria mercenaria*	Hard-shell clam	1.66E−030
15612	255	1993	Myosin heavy chain, striated muscle-like	*Aplysia californica*	Californian sea hare	9.36E−031
18456	149	1981	Actin subfamily protein	*Acanthamoeba castellanii*	Soil amoebae	3.23E−013
2367	1265	1673	Elongation factor 1 alpha	*Mytilus galloprovincialis*	Mediterranean mussel	0
15826	245	1541	Transcript Antisense to Ribosomal RNA (Tar1p)	*Medicago truncatula*	Barrel clover	3.48E−017
433	2216	1533	NADH dehydrogenase subunit 2 (mitochondrion)	*Mya arenaria*	Soft-shelled clam	7.77155E−94
16924	203	1424	Calponin-2	*Crassostrea gigas*	Pacific oyster	9.27E−013
209	2646	1354	Protein disulfide-isomerase	*Crassostrea gigas*	Pacific oyster	1.23E−173
619	1969	1341	Arginine kinase	*Pholas orientalis*	Oriental angel wing	0
12154	439	1280	Ribosomal protein rps12	*Eurythoe complanata*	Fire worm	1.81E−056
190	2707	1243	Myosin heavy chain, striated muscle-like	*Aplysia californica*	Californian sea hare	0
19872	107	1227	Actin-4	*Toxocara canis*	Dog roundworm	3.03E−011
3040	1140	1200	Myosin heavy chain	*Pecten maximus*	King scallop	2.55E−096
13067	381	1197	Transcript antisense to ribosomal RNA (Tar1p)	*Medicago truncatula*	Barrel clover	7.13255E−18
4048	1004	1161	Myosin heavy chain, striated muscle	*Crassostrea gigas*	Pacific oyster	1.09E−121
12702	401	1042	Ligand-gated ion channel 4-like	*Aplysia californica*	Californian sea hare	6.99E−013
19227	124	1041	Myosin, regulatory light chain	*Macrocallista nimbosa*	Sunray venus clam	1.21E−012
187	2730	1030	Heat shock protein HSP 90-alpha 1	*Crassostrea gigas*	Pacific oyster	0
1953	1363	1002	Fructose-1, 6-bisphosphate aldolase	*Meretrix meretrix*	Orient clam	1.19E−077
5581	846	993	60S ribosomal protein L4	*Crassostrea gigas*	Pacific oyster	3.00803E−129
15404	264	979	Cytochrome c oxidase subunit III (mitochondrion)	*Mya arenaria*	Soft-shelled clam	1.14E−031
17523	181	963	Cytochrome c oxidase subunit III (mitochondrion)	*Mya arenaria*	Soft-shelled clam	2.93134E−19
16470	221	960	Calponin-3	*Pinctada fucata*	Pearl oyster	8.72E−013
5696	836	950	Cytochrome c oxidase subunit I (mitochondrion)	*Mya arenaria*	Soft-shelled clam	1.93028e−120
15046	280	944	Myosin heavy chain	*Argopecten irradians*	Atlantic bay scallop	3.17082E−18
15886	243	943	Myosin, essential light chain	*Mercenaria mercenaria*	Hard-shell clam	1.12192E−15
7264	717	919	Beta-actin	*Meretrix meretrix*	Orient clam	7.06472E−133
1680	1435	903	Tubulin alpha-1 chain	*Harpegnathos saltator*	Indian jumping ant	0
13124	378	870	Tropomyosin	*Tresus keenae*	Horse clam	5.07894E−48
495	2111	826	Polyadenylate-binding protein 4	*Crassostrea gigas*	Pacific oyster	0
11402	478	812	NADH dehydrogenase subunit 1 (mitochondrion)	*Mya arenaria*	Soft-shelled clam	1.27497E−35
162	2807	787	Phosphoenolpyruvate carboxykinase [GTP]	*Crassostrea gigas*	Pacific oyster	0
4251	980	775	NADH dehydrogenase subunit 5 (mitochondrion)	*Mya arenaria*	Soft-shelled clam	9.23E−110
211	2639	771	Tyrosinase (tyr-3)	*Crassostrea gigas*	Pacific oyster	4.33E−086
268	2492	741	Heat shock protein 70	*Corbicula fluminea*	Golden clam	0
7748	686	734	60S ribosomal protein	*Aplysia californica*	Californian sea hare	2.16E−088
1122	1641	729	Voltage-dependent anion channel 2	*Haliotis diversicolor*	Many-coloured abalone	1.26E−095
10131	550	713	60S ribosomal protein L4	*Crassostrea gigas*	Pacific oyster	6.82E−022
2645	1207	694	Receptor for activated protein kinase	*Scrobicularia plana*	Peppery furrow shell	1.44E−169
10039	555	689	NADH dehydrogenase subunit 1 (mitochondrion)	*Mya arenaria*	Soft-shelled clam	1.81E−033
2970	1152	687	Cytochrome b (mitochondrion)	*Mya arenaria*	Soft-shelled clam	2.93E−140
3020	1144	672	ADP,ATP carrier protein	*Crassostrea gigas*	Pacific oyster	7.38E−136

the remaining tissues tested (except siphon for 16470 and 395) were equal to zero.

4. Discussion

4.1. M. truncata mantle transcriptome

Presented here is the first substantial molecular resource for *M. truncata*, which is a valuable resource for biomineralisation and comparative studies. The *M. truncata* mantle transcriptome was similar in size (~20,000 contigs), composition of most highly expressed transcripts and percentage annotation to other previously characterised bivalve mantle transcriptomes (Clark et al., 2010; Freer et al., 2014; Joubert et al., 2010; Niu et al., 2013; Shi et al., 2013); in particular it shares some consistent features with that of the Antarctic clam *L. elliptica*. When the *M. truncata* and *L. elliptica* mantle transcriptomes were compared using tBlastx, 17.35% of contigs were shared (below an E-value of 1E−10) representing a highly conserved core set of genes (Clark et al., 2010; Sleight et al., 2015). Both the *M. truncata* and *L. elliptica* mantle transcriptomes were heavily dominated by muscle related genes (Table 2; *Myosin*, *Actin* etc.), reflecting the contractile nature of this organ. In addition, putative mitochondrial respiratory chain genes (*NADH dehygrogenase*, *Cytochrome c*, *Arginine kinase* etc) were highly expressed in both, demonstrating that the mantle is a metabolically and transcriptionally active tissue. To date, our research has concentrated on *L. elliptica* and *M. truncata* has been chosen as a northern hemisphere, temperate comparison. *M. truncata* is often reported as an Arctic bivalve (Camus et al., 2002; Gillis and Ballantyne, 1999), however animals in the present study were sampled from a more southerly latitude, and hence much warmer region of their distribution on the North West coast of Scotland. *M. truncata* and *L. elliptica* are ecologically and morphologically very similar, but their physical environments (Arctic to temperate versus Antarctic), geographical extent (ranging from Arctic through subboreal to temperate versus Southern Ocean

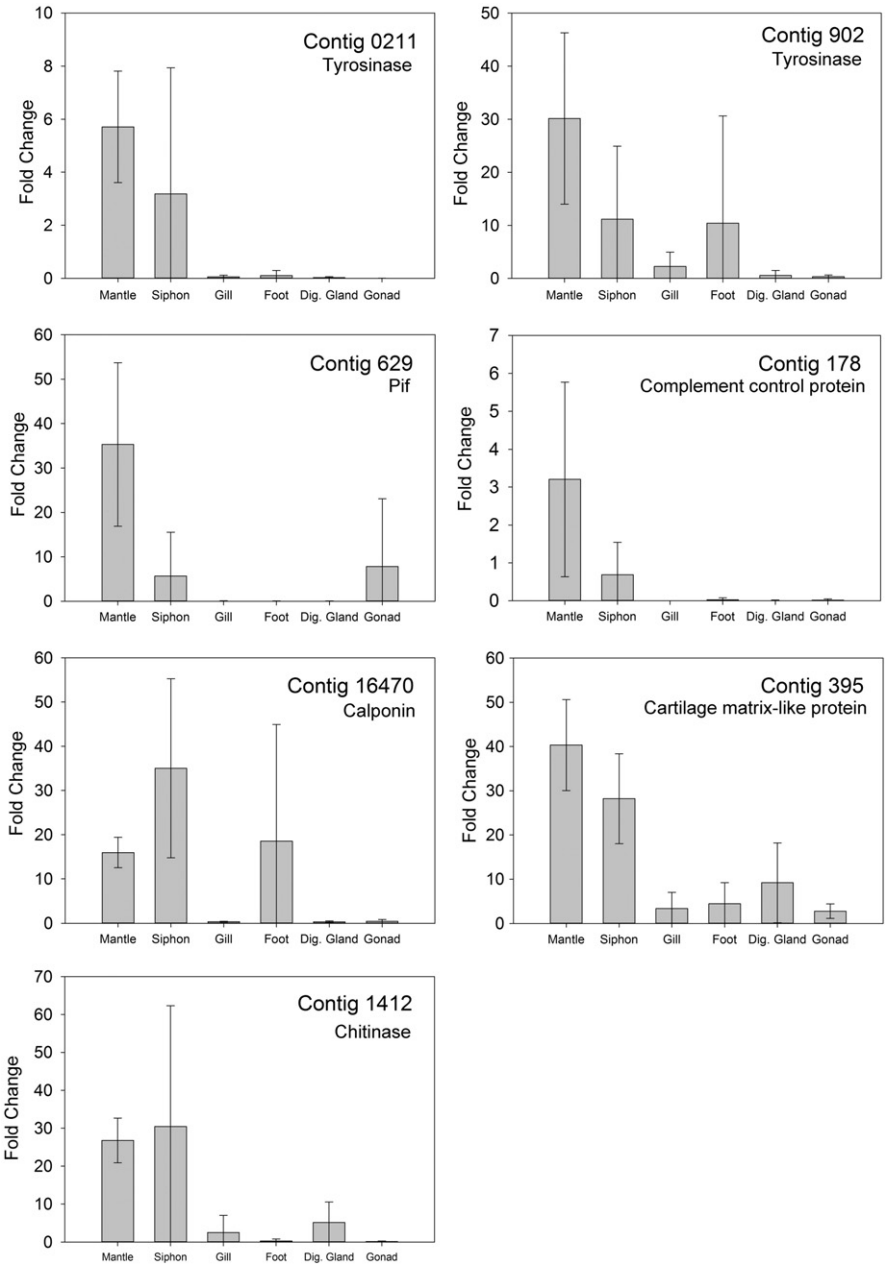

Fig. 3. Tissue distribution expression patterns of candidate biomineralisation genes determined via Q-PCR (mean average fold change ± 95% confidence intervals). Fold change calculated as $2^{-\Delta\Delta CT}$ using *Ribosomal 18s* as an internal housekeeping gene.

exclusively) and evolutionary history (phylogenetically distant relatives) differ significantly. In addition, the two species have different shell microstructures. As a result of their independent evolutionary trajectories in dissimilar physical conditions, with diverse selection pressures, *M. truncata* which inhabit temperate regions have a higher metabolic rate and shorter lifespan than *L. elliptica* (Camus et al., 2003, 2005; Peck et al., 2002; Philipp and Abele, 2010).

As well as sharing a core set of highly conserved genes, the *M. truncata* and *L. elliptica* most highly expressed mantle transcripts share more specific similarities at the individual gene level. Here we will focus on the genes likely to be involved in biomineralisation. Both transcriptomes have a single *Tyrosinase* gene in the most highly expressed set of transcripts, *L. elliptica* has *Tyrosinase B* and *M. truncata* has *Tyrosinase A3*. Tyrosinase is a biomineralisation protein involved in the formation of the shell matrix and periostracum (Huning et al., 2013; Sánchez-Ferrer et al., 1995; Zhang et al., 2006), its extreme high expression in the mantle organ of both clam species provides further evidence for its important role in shell deposition. A less well characterised biomineralisation candidate is Calponin, both species have two *Calponin* genes in the mostly highly expressed transcripts. Calponin proteins are typically involved in muscle contraction and interact closely with other muscle action proteins such as Actin and Myosin (Matthew et al., 2000). Its role in muscle contraction however, is thought to be primarily cross-linking and stabilisation of the muscle fibres (Jensen et al., 2014), and we hypothesise it could play a similar role in the stabilisation of the shell protein matrix. Several pieces of evidence support this idea: 1.) It is highly expressed at the transcript level in the mantle of the two clam species and a species of pearl oyster, *Pinctada martensii* (Shi et al., 2013). 2.) It has been demonstrated to be involved in the biomineralisation of bone in humans (Ueda et al., 2002). 3.) The shell matrix protein, PFMG8, has been shown (in silico) to contain a Calponin domain which has a calcium binding site (Evans, 2012). 4.) It has a mantle specific expression pattern (Fig. 3) and finally, 5.) Calponin proteins were found in both the shell and mantle proteome of *M. truncata* where it may interact with Myosin and contribute to shell elasticity (Arivalagan et al., 2016 — in this issue).

One noticeable difference between the *M. truncata* and *L. elliptica* mantle transcriptomes concerns the constitutive expression of heat shock proteins (HSPs). HSPs are involved in protein-folding and chaperoning and are either constitutively expressed, or induced in response to stress (Hartl, 1996). Both *Heat shock protein 70* (*Hsp70*) and *Heat shock protein 90-alpha* (*Hsp90*) were highly expressed in the *M. truncata* mantle, where as in *L. elliptica* there was no high expression of any HSP family members (above 300 reads — which was the cut-off used by Clark et al., 2010). *Hsp70* is classically regarded as inducible, rather than constitutive, and forms part of a classic "stress" response in many organisms (Clark et al., 2008; Clark and Peck, 2009). One possible explanation for the high background expression of inducible *Hsp70* in *M. truncata* is that the animals in the present study were sampled from a southerly latitude and warm region of their global distribution (summer sea surface temperatures in Dunstaffnage Bay have been recorded >14 °C) where they are close to their upper thermal tolerance (Amaro et al., 2005). Work by Amaro et al. (2005) demonstrated that *M. truncata* at its southern distribution limit (the Frisian Front in the North Sea experiencing water temperatures >14 °C) have low numbers of ripe oocytes and frequent years of poor recruitment, indicating the southern populations could be in a constant state of low-level thermal stress. *Hsp90* on the other hand, is thought of as a constitutively expressed protein, and its high expression in the *M. truncata* mantle transcriptome is likely to represent normal cellular processes in the mantle, similar to other invertebrate species (Huang et al., 2013).

4.2. Tyrosinase bivalve phylogeny

Tyrosinase is a multifunctional well-characterised, shell-associated protein which has been shown to have a functional role in the cross-linking of the soluble periostracum precursor (the periostracin) to form an insoluble periostracum (Waite et al., 1979); to be localised in the prismatic layer of shell (Nagai et al., 2007) and to be expressed in the pallial mantle and hence involved in the nacreous layer of the shell (Takgi and Miyashita, 2014). In addition, Tyrosinase is involved in numerous other biological processes such as innate immunity, pigmentation and wound healing (Aguilera et al., 2014; Zhang et al., 2006). We have identified at least five gene copies of *Tyrosinase* in the *M. truncata* mantle transcriptome which are likely to be a result of several gene duplication events followed by sub-functionalisation (Force et al., 1999). It is possible that an expansion and subsequent sub-functionalisation has produced Tyrosinase paralogues which have completely new functions besides shell formation, for example in the immune system, as suggested by Wang et al. (2009) and Esposito et al. (2012). Given the well-characterised and clearly important nature of Tyrosinase in molluscan shell formation, it is important to investigate its evolution in order to better understand how mollusc shell is produced between species. *M. truncata* Tyrosinase amino acid sequences were therefore investigated within a phylogenetic context. Similar to Aguilera et al. (2014) and other previous Tyrosinase phylogenies (Aguilera et al., 2013), many of the nodes had low support values (Fig. 2, Supplementary Figs. 1, 2 and 3). Adding *M. truncata* sequence data to three independent phylogenetic analyses did not alter the overall tree topology and the major patterns described by Aguilera and colleagues were largely still resolved — further validating their work.

Four of the five *M. truncata* Tyrosinase amino acid sequences formed a well-supported cluster with *L. elliptica* Tyrosinase B. It is possible this cluster represents an expansion within the *M. truncata* genome. The fifth *M. truncata* sequence grouped with Tyrosinase A3 sequences from *C. gigas* and *P. fucata*. Given that one of the *L. elliptica* sequences group with the *M. truncata* sequences it is likely they have evolved under at least some similar selection pressures with regard to shell growth. *M. truncata* however, show evidence for a Tyrosinase expansion, which is absent in *L. elliptica*. Antarctic marine invertebrates are largely stenothermal due to evolution at constant cold temperatures for long periods of geological time (Rogers, 2007). We find that, for the *Tyrosinase* gene family, Antarctic clams are less diverse than their temperate counterparts *M. truncata*, and other marine shelled-molluscs. An explanation for higher Tyrosinase diversity in *M. truncata* than *L. elliptica* could be due to *M. truncata's* wider geographical distribution and spread over environmental gradients. As a species, *M. truncata* could require more diverse molecular machinery to cope with the diverse environments they inhabit; supporting the hypothesis that diversity is positively correlated to environmental heterogeneity and stress (Nevo, 2001; Van Valen, 1965).

4.3. Tissue distribution of biomineralisation gene expression

As expected, all of the putative biomineralisation candidate genes we selected for tissue distribution analysis (Table 1) showed a mantle/siphon-specific expression pattern (Fig. 3). Tyrosinase and Pif are well characterised shell proteins (Nagai et al., 2007; Suzuki et al., 2009); they have recently been shown to respond to shell damage in *L. elliptica* (Sleight et al., 2015), and the mantle/siphon specific expression patterns found in *M. truncata* provide further evidence to support their hypothesised functional role in shell deposition in the two clam species. Calponin is likely to be involved in biomineralisation (as discussed at length in Section 4.1) however, like many biomineralisation proteins, it is multi-functional and also involved in muscle contraction where it interacts with Myosin and hence it also showed variable expression in the foot (a muscle). Cartilage matrix proteins are involved in calcium phosphate biomineralisation in vertebrates where they bind to calcium phosphate crystals and form part of an extracellular matrix (Acharya et al., 2014). Arivalagan et al. (2016 — in this issue) identified Cartilage matrix protein in the *M. truncata* shell proteome, and taken together with the mantle-specific gene expression

pattern found in the present study, it is likely to play a similar matrix-like role in mollusc biomineralisation. Chitinase is an enzyme hypothesised to be involved in mollusc shell matrix construction (Sleight et al., 2015), as well as immunity (Badariotti et al., 2007). The function of Chitinase and Chitinase-like proteins have been investigated in arthropods with chitinous exoskeletons; they are typically involved in moult-cycles, wound healing and tissue repair (Bonneh-Barkay et al., 2010; Chen et al., 2004), however their exact function in the mollusc shell matrix is still unclear. Previous work shows *Chitinase* expression is up regulated in response to injury after 21 days in young, but not old, *L. elliptica* (Husmann et al., 2014); and Sleight et al. (2015) also found variable expression in *L. elliptica* over time in response to shell damage. Very high expression was found in young damaged animals after one week, whereas no expression was detected in control or damaged adult animals. The mantle specific expression pattern found in the present study, as well as Chitinase presence in the *M. truncata* shell proteome (Arivalagan et al., 2016 — in this issue), provides further support for its active involvement in shell deposition. More research is required to understand its hugely variable expression in young versus old animals and its exact function during matrix formation and shell secretion.

Complement control proteins are multifunctional and involved in both the immune system (Ferreira et al., 2010) and possibly biomineralisation (Arivalagan et al., 2016 — in this issue). Bivalve shell and mantle combined act as a barrier to the external environment, and as such are likely to be entwined with immune processes. Disentangling immune and biomineralisation mechanisms represents a significant challenge for researchers trying to understand how molluscs build their shells. The challenge is partly due to the dual role of haemocytes both as immune cells and hypothesised calcium carbonate chaperones (Mount et al., 2004). In addition to the observed mantle specific expression of *Complement control protein* in the present study and previous reports of immune genes such as *Mytilin* responding to damage in *L. elliptica* (Sleight et al., 2015), Arivalagan et al. (2016 — in this issue) found immune proteins in the *M. truncata* shell proteome (and verified their presence was not due to contamination). The expression of immune genes in the *M. truncata* mantle, as well as the immune proteins found in its shell, could be explained in several ways: 1.) general haemocyte circulation in the mantle could result in coincidental incorporation into the shell as an accidental bi-product of their immune function (as per the mantle's role as a barrier); 2.) whilst haemocytes actively deposit calcium carbonate to the shell secretion site they could be coincidentally trapped in the shell matrix space, as an accidental bi-product of their role in biomineralisation, as proposed by Arivalagan et al. (2016 — in this issue); or 3.) immune proteins could serve a genuine dual-functional role, both in aiding biomineralisaion during calcium carbonate secretion from haemocytes, and possibly also at a structural matrix-level, as well as fighting infection as an anti-microbial peptide in the shell, and in the circulating haemocytes in the mantle.

5. Conclusion

We present the first substantial molecular resource for *M. truncata*. The mantle transcriptome was 454-sequenced, de novo-assembled and BLAST sequence similarity-annotated to produce a total of 20,106 contigs, of which approximately 19% were assigned putative functions. The mantle transcriptomes of *M. truncata* and the Antarctic clam (*L. elliptica*) were compared using tBLASTx and overall, shared a core complement (17%) of highly conserved transcripts. Looking at the most highly expressed genes in the two species showed that many of the dominant biological functions (contraction, energy production, biomineralisation) were conserved. The Tyrosinase proteins from *M. truncata* were analysed phylogenetically and showed a small expansion which was closely related to *L. elliptica*, however *M. truncata* had more diversity in Tyrosinase proteins. The tissue distribution expression pattern of candidate biomineralisation genes was investigated using Q-PCR, all genes showed a mantle specific expression pattern supporting their hypothesised role in shell secretion. We provide very preliminary insights on how clams in different conditions (temperate versus polar) build their shells — a topic which we will continue to pursue in our research group. In addition, we provide a valuable molecular resource for future comparative studies investigating biomineralisation.

Supplementary data to this article can be found online at http://dx.doi.org/10.1016/j.margen.2016.01.003.

Acknowledgements

VAS was funded by a NERC DTG studentship (Project Reference: NE/J500173/1) to the British Antarctic Survey. MSC, MAST and LSP were financed by NERC core funding to the British Antarctic Survey, Polar Sciences for Planet Earth Programme. JA was funded by the European Union Seventh Framework Programme under grant agreement no. 605051. We would like to thank Laura J. Weir for technical assistance, Elizabeth M. Harper for advice on shell microstructure and Felipe Aguilera for providing a molluscan Tyrosinase alignment. We thank the dive team at the NERC National Centre for Scientific Diving, Oban for animal collection and Dr Kim Last at the Scottish Association for Marine Science for overseeing animal husbandry.

References

Acharya, C., Yik, J.H.N., Kishore, A., Dinh, V.V., Di Cesare, P.E., Haudenschild, D.R., 2014. Cartilage oligomeric matrix protein and its binding partners in the cartilage extracellular matrix: interaction, regulation and role in chondrogenesis. Matrix Biol. 37, 102–111.
Addadi, L., Weiner, S., 1997. Biomineralization: a pavement of pearl. Nature 389, 912–915.
Aguilera, F., McDougall, C., Degnan, B., 2013. Origin, evolution and classification of type-3 copper proteins: lineage-specific gene expansions and losses across the Metazoa. BMC Evol. Biol. 13, 96.
Aguilera, F., McDougall, C., Degnan, B.M., 2014. Evolution of the tyrosinase gene family in bivalve molluscs: independent expansion of the mantle gene repertoire. Acta biomater. 10, 3855–3865.
Altschul, S.F., Gish, W., Miller, W., Myers, E.W., Lipman, D.J., 1990. Basic local alignment search tool. J. Mol. Biol. 215, 403–410.
Amaro, T., Duineveld, G., Tyler, P., 2005. Does *Mya truncata* reproduce at its southern distribution limit? Preliminary information. J. Shellfish Res. 24, 25–28.
Arivalagan, J., Marie, B., Sleight, V.A., Clark, M.S., Berland, S., Marie, A., 2016. Shell matrix proteins of the clam, *Mya truncata*: roles beyond shell formation through proteomic study. Mar. Genomics 27, 69–74 (in this issue).
Badariotti, F., Thuau, R., Lelong, C., Dubos, M.P., Favrel, P., 2007. Characterization of an atypical family 18 chitinase from the oyster *Crassostrea gigas*: evidence for a role in early development and immunity. Dev. Comp. Immunol. 31, 559–570.
Bieler, R., Mikkelsen, P.M., Collins, T.M., Glover, E.A., Gonzalez, V.L., Graf, D.L., Harper, E.M., Healy, J., Kawauchi, G.Y., Sharma, P.P., Staubach, S., Strong, E.E., Taylor, J.D., Temkin, I., Zardus, J.D., Clark, S., Guzman, A., McIntyre, E., Sharp, P., Giribet, G., 2014. Investigating the bivalve tree of life — an exemplar-based approach combining molecular and novel morphological characters. Invertebr. Syst. 28, 32–115.
Bonneh-Barkay, D., Zagadailov, P., Zou, H.C., Niyonkuru, C., Figley, M., Starkey, A., Wang, G.J., Bissel, S.J., Wiley, C.A., Wagner, A.K., 2010. YKL-40 expression in traumatic brain injury: an initial analysis. J. Neurotrauma 27, 1215–1223.
Camus, L., Richardsen, S.R., Borseth, J.F., Grosvik, B.E., Gulliksen, B., Jones, M.B., Lonne, O.J., Regoli, F., Depledge, M.H., 2002. Biomarkers in the soft shell Arctic clam *Mya truncata*: seasonal variability and impact of PAH. Mar. Environ. Res. 54, 830.
Camus, L., Birkely, S.R., Jones, M.B., Borseth, J.F., Grosvik, B.E., Gulliksen, B., Lonne, O.J., Regoli, F., Depledge, M.H., 2003. Biomarker responses and PAH uptake in *Mya truncata* following exposure to oil-contaminated sediment in an Arctic fjord (Svalbard). Sci. Total Environ. 308, 221–234.
Camus, L., Gulliksen, B., Depledge, M.H., Jones, M.B., 2005. Polar bivalves are characterized by high antioxidant defences. Polar Res. 24, 111–118.
Castresana, J., 2000. Selection of conserved blocks from multiple alignments for their use in phylogenetic analysis. Mol. Biol. Evol. 17, 540–552.
Chen, L., Wu, W., Dentchev, T., Zeng, Y., Wang, J.H., Tsui, I., Tobias, J.W., Bennett, J., Baldwin, D., Dunaief, J.L., 2004. Light damage induced changes in mouse retinal gene expression. Exp. Eye Res. 79, 239–247.
Clark, M.S., Peck, L.S., 2009. HSP70 heat shock proteins and environmental stress in Antarctic marine organisms: a mini-review. Mar. Genomics 2, 11–18.
Clark, M.S., Fraser, K.P., Peck, L., 2008. Antarctic marine molluscs do have an HSP70 heat shock response. Cell Stress Chaperones 13, 39–49.
Clark, M.S., Thorne, M.A.S., Vieira, F.A., Cardoso, J.C.R., Power, D.M., Peck, L.S., 2010. Insights into shell deposition in the Antarctic bivalve *Laternula elliptica*: gene discovery in the mantle transcriptome using 454 pyrosequencing. BMC Genomics 11.
Esposito, R., D'Aniello, S., Squarzoni, P., Pezzotti, M.R., Ristoratore, F., Spagnuolo, A., 2012. New insights into the evolution of metazoan tyrosinase gene family. PLoS ONE 7, e35731.
Evans, J.S., 2012. Aragonite-associated biomineralization proteins are disordered and contain interactive motifs. Bioinformatics 28, 3182–3185.

Ferreira, V.P., Pangburn, M.K., Cortes, C., 2010. Complement control protein factor H: the good, the bad, and the inadequate. Mol. Immunol. 47, 2187–2197.
Force, A., Lynch, M., Pickett, F.B., Amores, A., Yan, Y.L., Postlethwait, J., 1999. Preservation of duplicate genes by complementary, degenerative mutations. Genetics 151, 1531–1545.
Freer, A., Bridgett, S., Jiang, J.H., Cusack, M., 2014. Biomineral proteins from *Mytilus edulis* mantle tissue transcriptome. Mar. Biotechnol. 16, 34–45.
Gillis, T.E., Ballantyne, J.S., 1999. Mitochondrial membrane composition of two arctic marine bivalve mollusks, *Serripes groenlandicus* and *Mya truncata*. Lipids 34, 53–57.
Hartl, F.U., 1996. Molecular chaperones in cellular protein folding. Nature 381, 571–580.
Huang, A.-M., Geng, Y., Wang, K.-Y., Zeng, F., Liu, Q., Wang, Y., Sun, Y., Liu, X.-X., Zhou, Y., 2013. Molecular cloning and expression analysis of heat shock protein 90 (Hsp90) of the mud crab, *Scylla paramamosain*. J. Agric. Sci. 5 (7).
Huning, A., Melzner, F., Thomsen, J., Gutowska, M.A., Kramer, L., Frickenhaus, S., Rosenstiel, P., Portner, H.O., Philipp, E.E.R., Lucassen, M., 2013. Impacts of seawater acidification on mantle gene expression patterns of the Baltic Sea blue mussel: implications for shell formation and energy metabolism. Mar. Biol. 160, 1845–1861.
Husmann, G., Abele, D., Rosenstiel, P., Clark, M.S., Kraemer, L., Philipp, E.E.R., 2014. Age-dependent expression of stress and antimicrobial genes in the hemocytes and siphon tissue of the Antarctic bivalve, *Laternula elliptica*, exposed to injury and starvation. Cell Stress Chaperones 19, 15–32.
Jackson, D.J., McDougall, C., Woodcroft, B., Moase, P., Rose, R.A., Kube, M., Reinhardt, R., Rokhsar, D.S., Montagnani, C., Joubert, C., Piquemal, D., Degnan, B.M., 2010. Parallel evolution of nacre building gene sets in molluscs. Mol. Biol. Evol. 27, 591–608.
Jensen, M.H., Morris, E.J., Gallant, C.M., Morgan, K.G., Weitz, D.A., Moore, J.R., 2014. Mechanism of calponin stabilization of cross-linked actin networks. Biophys. J. 106, 793–800.
Joubert, C., Piquemal, D., Marie, B., Manchon, L., Pierrat, F., Zanella-Cleon, I., Cochennec-Laureau, N., Gueguen, Y., Montagnani, C., 2010. Transcriptome and proteome analysis of *Pinctada margaritifera* calcifying mantle and shell: focus on biomineralization. BMC Genomics 11.
Katoh, K., Kuma, K., Toh, H., Miyata, T., 2005. MAFFT version 5: improvement in accuracy of multiple sequence alignment. Nucleic Acids Res. 33, 511–518.
Larkin, M.A., Blackshields, G., Brown, N.P., Chenna, R., McGettigan, P.A., McWilliam, H., Valentin, F., Wallace, I.M., Wilm, A., Lopez, R., Thompson, J.D., Gibson, T.J., Higgins, D.G., 2007. Clustal W and Clustal X version 2.0. Bioinformatics 23, 2947–2948.
Marie, B., Marie, A., Jackson, D.J., Dubost, L., Degnan, B.M., Milet, C., Marin, F., 2010. Proteomic analysis of the organic matrix of the abalone *Haliotis asinina* calcified shell. Proteome Sci. 8.
Marie, B., Jackson, D.J., Ramos-Silva, P., Zanella-Cleon, I., Guichard, N., Marin, F., 2013. The shell-forming proteome of *Lottia gigantea* reveals both deep conservations and lineage-specific novelties. FEBS J. 280, 214–232.
Marin, F., Luquet, G., 2004. Molluscan shell proteins. C.R. Palevol 3, 469–492.
Matthew, J.D., Khromov, A.S., McDuffie, M.J., Somlyo, A.V., Somlyo, A.P., Taniguchi, S., Takahashi, K., 2000. Contractile properties and proteins of smooth muscles of a calponin knockout mouse. J. Physiol. 529 (Pt 3), 811–824.
Meenakshi, V.R., Hare, P.E., Wilbur, K.M., 1971. Amino acids of the organic matrix of neogastropod shells. Comp. Biochem. Physiol. B Comp. Biochem. 40, 1037–1043.
Morley, S., Peck, L., Tan, K., Martin, S., Portner, H., 2007. Slowest of the slow: latitudinal insensitivity of burrowing capacity in the bivalve *Laternula*. Mar. Biol. 151, 1823–1830.
Mount, A.S., Wheeler, A.P., Paradkar, R.P., Snider, D., 2004. Hemocyte-mediated shell mineralization in the eastern oyster. Science 304, 297–300.
Nagai, K., Yano, M., Morimoto, K., Miyamoto, H., 2007. Tyrosinase localization in mollusc shells. Comp. Biochem. Physiol. B Biochem. Mol. Biol. 146, 207–214.
Nevo, E., 2001. Evolution of genome–phenome diversity under environmental stress. Proc. Natl. Acad. Sci. 98, 6233–6240.
Niu, D.H., Wang, L., Sun, F.Y., Liu, Z.J., Li, J.L., 2013. Development of molecular resources for an intertidal clam, *Sinonovacula constricta*, using 454 transcriptome sequencing. Plos One 8.
Peck, L.S., Portner, H.O., Hardewig, I., 2002. Metabolic demand, oxygen supply, and critical temperatures in the antarctic bivalve *Laternula elliptica*. Physiol. Biochem. Zool. 75, 123–133.
Philipp, E.E.R., Abele, D., 2010. Masters of longevity: lessons from long-lived bivalves — a mini-review. Gerontology 56, 55–65.
Powers, S.P., Bishop, M.A., Grabowski, J.H., Peterson, C.H., 2006. Distribution of the invasive bivalve *Mya arenaria* L. on intertidal flats of southcentral Alaska. J. Sea Res. 55, 207–216.
Queirós, A.M., Birchenough, S.N.R., Bremner, J., Godbold, J.A., Parker, Ruth E., Romero-Ramirez, A., Reiss, H., Solan, M., Somerfield, P.J., Van Colen, C., Van Hoey, G., Widdicombe, S., 2013. A bioturbation classification of European marine infaunal invertebrates. Ecol. Evol 3, 3958–3985.
Rogers, A.D., 2007. Evolution and biodiversity of Antarctic organisms: a molecular perspective. Philos. Trans. R. Soc. B 362, 2191–2214.
Ronquist, F., Teslenko, M., van der Mark, P., Ayres, D.L., Darling, A., Hohna, S., Larget, B., Liu, L., Suchard, M.A., Huelsenbeck, J.P., 2012. MrBayes 3.2: efficient bayesian phylogenetic inference and model choice across a large model space. Syst. Biol. 61, 539–542.
Sánchez-Ferrer, Á., Neptuno Rodríguez-López, J., García-Cánovas, F., García-Carmona, F., 1995. Tyrosinase: a comprehensive review of its mechanism. Biochim. Biophys. Acta Protein Struct. Mol. Enzymol. 1247, 1–11.
Shi, Y., Yu, C., Gu, Z., Zhan, X., Wang, Y., Wang, A., 2013. Characterization of the pearl oyster (*Pinctada martensii*) mantle transcriptome unravels biomineralization genes. Mar. Biotechnol. 15, 175–187.
Siah, A., Dohoo, C., McKenna, P., Delaporte, M., Berthe, F.C.J., 2008. Selecting a set of housekeeping genes for quantitative real-time PCR in normal and tetraploid haemocytes of soft-shell clams, *Mya arenaria*. Fish Shellfish Immunol. 25, 202–207.
Silvestro, D., Michalak, I., 2012. raxmlGUI: a graphical front-end for RAxML. Org. Divers. Evol. 12, 335–337.
Sleight, V.A., Thorne, M.A., Peck, L.S., Clark, M.S., 2015. Transcriptomic response to shell damage in the Antarctic clam, *Laternula elliptica*: time scales and spatial localisation. Mar. Genomics 20, 45–55.
Sousa, R., Gutierrez, J.L., Aldridge, D.C., 2009. Non-indigenous invasive bivalves as ecosystem engineers. Biol. Invasions 11, 2367–2385.
Suzuki, M., Saruwatari, K., Kogure, T., Yamamoto, Y., Nishimura, T., Kato, T., Nagasawa, H., 2009. An acidic matrix protein, Pif, is a key macromolecule for nacre formation. Science 325, 1388–1390.
Takgi, R., Miyashita, T., 2014. A cDNA cloning of a novel alpha-class tyrosinase of *Pinctada fucata*: its expression analysis and characterization of the expressed protein. Enzym. Res. 2014, 9.
Tamura, K., Peterson, D., Peterson, N., Stecher, G., Nei, M., Kumar, S., 2011. MEGA5: molecular evolutionary genetics analysis using maximum likelihood, evolutionary distance, and maximum parsimony methods. Mol. Biol. Evol. 28, 2731–2739.
Thompson, J.D., Thierry, J.C., Poch, O., 2003. RASCAL: rapid scanning and correction of multiple sequence alignments. Bioinformatics 19, 1155–1161.
Ueda, T., Araki, N., Mano, M., Myoui, A., Joyama, S., Ishiguro, S., Yamamura, H., Takahashi, K., Kudawara, I., Yoshikawa, H., 2002. Frequent expression of smooth muscle markers in malignant fibrous histiocytoma of bone. J. Clin. Pathol. 55, 853–858.
Van Valen, L., 1965. Morphological variation and width of ecological niche. Am. Nat. 377–390.
Vermeij, G.J., 2005. Shells inside out: the architecture, evolution and function of shell envelopment in molluscs. Evolving Form Function Fossils Dev. 197–221.
Waite, J.H., Saleuddin, A.S.M., Andersen, S.O., 1979. Periostracin — a soluble precursor of sclerotized periostracum in *Mytilus edulis L.* J. Comp. Physiol. B 130, 301–307.
Wang, T., Sun, Y., Jin, L., Xu, Y., Wang, L., Ren, T., Wang, K., 2009. Enhancement of non-specific immune response in sea cucumber (*Apostichopus japonicus*) by *Astragalus membranaceus* and its polysaccharides. Fish Shellfish Immunol. 27, 757–762.
Weiner, S., Hood, L., 1975. Soluble protein of the organic matrix of mollusk shells: a potential template for shell formation. Science 190, 987–989.
Werner, G.D.A., Gemmell, P., Grosser, S., Hamer, R., Shimeld, S.M., 2013. Analysis of a deep transcriptome from the mantle tissue of *Patella vulgata* Linnaeus (Mollusca: Gastropoda: Patellidae) reveals candidate biomineralising genes. Mar. Biotechnol. 15, 230–243.
Ye, J., Coulouris, G., Zaretskaya, I., Cutcutache, I., Rozen, S., Madden, T.L., 2012. Primer-BLAST: a tool to design target-specific primers for polymerase chain reaction. BMC Bioinforma. 13, 134.
Zhang, C., Xie, L.P., Huang, J., Chen, L., Zhang, R.Q., 2006. A novel putative tyrosinase involved in periostracum formation from the pearl oyster (*Pinctada fucata*). Biochem. Biophys. Res. Commun. 342, 632–639.
Zhang, G., Fang, X., Guo, X., Li, L., Luo, R., Xu, F., Yang, P., Zhang, L., Wang, X., Qi, H., Xiong, Z., Que, H., Xie, Y., Holland, P.W.H., Paps, J., Zhu, Y., Wu, F., Chen, Y., Wang, J., Peng, C., Meng, J., Yang, L., Liu, J., Wen, B., Zhang, N., Huang, Z., Zhu, Q., Feng, Y., Mount, A., Hedgecock, D., Xu, Z., Liu, Y., Domazet-Loso, T., Du, Y., Sun, X., Zhang, S., Liu, B., Cheng, P., Jiang, X., Li, J., Fan, D., Wang, W., Fu, W., Wang, T., Wang, B., Zhang, J., Peng, Z., Li, Y., Li, N., Wang, J., Chen, M., He, Y., Tan, F., Song, X., Zheng, Q., Huang, R., Yang, H., Du, X., Chen, L., Yang, M., Gaffney, P.M., Wang, S., Luo, L., She, Z., Ming, Y., Huang, W., Zhang, S., Huang, B., Zhang, Y., Qu, T., Ni, P., Miao, G., Wang, J., Wang, Q., Steinberg, C.E.W., Wang, H., Li, N., Qian, L., Zhang, G., Li, Y., Yang, H., Liu, X., Wang, J., Yin, Y., Wang, J., 2012. The oyster genome reveals stress adaptation and complexity of shell formation. Nature 490, 49–54.